DE-SC0002209:
Bridging the PSI Knowledge Gap: A Multi-Scale Approach

A final report submitted by:
Brian D. Wirth, PI
University of California, Berkeley (2002-2014)
University of Tennessee, Knoxville (2010-present)

Submitted to:
DOE Office of Fusion Energy Sciences

1. EXECUTIVE SUMMARY

Plasma-surface interactions (PSI) pose an immense scientific hurdle in magnetic confinement fusion and our present understanding of PSI in confinement environments is highly inadequate; indeed, a recent Fusion Energy Sciences Advisory Committee report found that 4 out of the 5 top five fusion knowledge gaps were related to PSI. The time is appropriate to develop a concentrated and synergistic science effort that would expand, exploit and integrate the wealth of laboratory ion-beam and plasma research, as well as exciting new computational tools, towards the goal of bridging the PSI knowledge gap. This effort would broadly advance plasma and material sciences, while providing critical knowledge towards progress in fusion PSI.

This project involves the development of a Science Center focused on a new approach to PSI science; an approach that both exploits access to state-of-the-art PSI experiments and modeling, as well as confinement devices. The organizing principle is to develop synergistic experimental and modeling tools that treat the truly coupled multi-scale aspect of the PSI issues in confinement devices. This is motivated by the simple observation that while typical lab experiments and models allow independent manipulation of controlling variables, the confinement PSI environment is essentially self-determined with few outside controls. This means that processes that may be treated independently in laboratory experiments, because they involve vastly different physical and time scales, will now affect one another in the confinement environment. Also, lab experiments cannot simultaneously match all exposure conditions found in confinement devices typically forcing a linear extrapolation of lab results. At the same time programmatic limitations prevent confinement experiments alone from answering many key PSI questions. The resolution to this problem is to usefully exploit access to PSI science in lab devices, while retooling our thinking from a linear and de-coupled extrapolation to a multi-scale, coupled approach.

The PSI Plasma Center consisted of three equal co-centers; one located at the MIT Plasma Science and Fusion Center, one at UC San Diego Center for Energy Research and one at the UC Berkeley Department of Nuclear Engineering, which moved to the University of Tennessee, Knoxville (UTK) with Professor Brian Wirth in July 2010. The Center had three co-directors: Prof. Dennis Whyte led the MIT co-center, the UCSD co-center was led by Dr. Russell Doerner, and Prof. Brian Wirth led the UCB/UTK center. The directors have extensive experience in PSI and material research, and have been internationally recognized in the magnetic fusion, materials and plasma research fields. The co-centers feature keystone PSI experimental and modeling facilities dedicated to PSI science: the DIONISOS/CLASS facility at MIT, the PISCES facility at UCSD, and the state-of-the-art numerical modeling capabilities at UCB/UTK. A collaborative partner in the center is Sandia National Laboratory at Livermore (SNL/CA), which has extensive capabilities with low energy ion beams and surface diagnostics, as well as supporting plasma facilities, including the Tritium Plasma Experiment, all of which significantly augment the Center. Interpretive, continuum material models are available through SNL/CA, UCSD and MIT. The participating institutions of MIT, UCSD, UCB/UTK, SNL/CA and LLNL brought a formidable array of experimental tools and personnel abilities into the PSI Plasma Center.

Our work has focused on modeling activities associated with plasma surface interactions that are involved in effects of He and H plasma bombardment on tungsten surfaces. This involved performing computational material modeling of the surface evolution during plasma bombardment using molecular dynamics modeling. The principal outcomes of the research efforts within the combined experimental – modeling PSI center are to provide a knowledgebase of the mechanisms of surface degradation, and the influence of the surface on plasma conditions.

2. MOTIVATION AND BACKGROUND

The performance demands on plasma-facing components (PFCs), first-wall and blanket systems of future fusion power plants are beyond the capability of current materials, which is one of the reasons that the United States National Academy of Engineering has ranked the quest for fusion as one of the top grand challenges for engineering in the 21st Century [1]. Furthermore, it is clear that the plasma-surface interactions (PSIs) occurring in the divertor and PFCs pose a critical scientific challenge that limits our ability to achieve electricity production from nuclear fusion. Indeed, it is well established that PSIs constitute critically important scientific issues for fusion power, and these issues affect the PFC lifetime, as well as core fusion plasma performance and the recycling of the hydrogen fuel. The literature on the subject goes back to the early 1960s [2,3] and entire conference series have been dedicated to the topic, such as the International Conference on Plasma Surface Interactions in Controlled Fusion [4]. Likewise, the conference series on the effects of hydrogen and helium interactions in materials goes back decades [5,6]. Comprehensive reviews of plasma materials interactions and high-heat-flux components include a 2001 article by Federici and co-authors [7] and a more recent 2010 article by Raffray and co-authors [8].

It is evident that three coupled spatial regions influence PFC materials evolution and performance [7-9]. These are (1) the edge and scrape-off layer region of the plasma, (2) the near-surface region where the material responsds to extreme thermal and particle fluxes under the influence of, and feedback to, the plasma sheath, and (3) the bulk structural materials region that responds to an intense, 14 MeV peaked neutron spectrum which produces very high concentrations of transmuted elements through (n,p) and (n,α) reactions and structural material

property degradation. The main focus of this article is on describing the challenges and opportunities for high-performance computing to contribute to our ability to understand and predict the materials science of surface evolution in mixed-material PFCs resulting from the particle and thermal particle fluxes from the plasma, and the impact on the core plasma and device performance. However, the coupled nature of these spatial domains necessitates the integration of modeling approaches for each domain in order to better evaluate the feedback between each region on the performance of the other more accurately. For example, a model of the interface of the surface and the plasma edge/scrapeoff layer is necessary to determine the incident particle and thermal fluxes that constitute the driving forces for PSI, as well as to account for the processes of excitation, ionization, and charge-exchange that can result in species re-deposition. Likewise, the interface between the surface and the bulk, where defect creation is no longer influenced by the presence of a free surface, is critical in determining the extent to which defect creation by high-energy neutrons impact retention and permeation of hydrogen isotopes, with a significant unknown existing with respect to the tritium permeation behavior in metallic PFC at elevated temperatures.

Gaining a physical understanding and establishing a predictive modeling capability in this critical PSI area requires that complex and diverse physics occurring over a wide range of length (Ångströms to meters) and time (femtoseconds to seconds, days to years) scales be addressed simultaneously, and that extensive physical processes across the plasma-surface-bulk materials interfaces be integrated. Figures 1 and 2 illustrate phenomena that govern the response of the materials surface to plasma exposure [9], and the computational models that must be accurately integrated. While vastly different length scales characterize the surface (~nm) and plasma

processes (~mm) as indicated in Fig. 1, the plasma and the material's surface are strongly coupled to each other, mediated by an electrostatic and magnetic sheath, through the nearly continuous exchange and recycling of incident ion and neutral species and the re-deposition of eroded particles. These interactions are more explicitly shown in Fig. 2, along with the corresponding time scales upon which they occur. These physical processes occur over a disparate range of time scales, which poses a challenge both to modeling, and experimental characterization of both the individual and coupled processes. As one example, the high probability (> 90%) of prompt local ionization and re-deposition of sputtered material atoms means that the surface material that is in contact with the plasma is itself a plasma-deposited surface, as opposed to the original well-ordered surface of the material that existed at the beginning of operation [9]. Likewise, the recycling of hydrogen plasma (fuel) is self-regulated through processes involving near-surface diffusion, trapping, and gas bubble formation, coupled to the ionization that results from interactions with the plasma. The multitude of time and length scales controlling material evolution and device performance requires the development not only of detailed physics models and computational strategies at each of these scales, but also of computational algorithms and methods to couple them strongly and in such a way that can be robustly and vigorously tested and validated. It is important in this regard that PFC simulation tools capture the kinetic evolution of defect and impurity species over diffusional timescales that are inaccessible through molecular dynamics (MD) techniques alone.

As helium, deuterium or tritium particles bombard the surface, they can reflect, induce sputtering of surface atoms, be adsorbed onto the surface, or implanted below the surface depending on the type of ion, and their kinetic energy and angle of incidence. Likewise, sputtered or eroded material from a surface can be ionized, transported through the plasma and re-deposited. Since

implantation energies are generally in the range of 10 to 1000 eV, the implantation depth is generally only a few nanometers. As more implanted particles accumulate within the surface layer, eventually a steady-state condition can result, in which the flux of species implanted into the materials is balanced by that released from the material. The extent to which both surface morphology and sub-surface defect creation and evolution processes driven by neutron-induced damage influence the diffusion, trapping and precipitation of hydrogen and helium species into gas bubbles is an outstanding question that impacts the tritium permeation, retention and near-surface saturation levels.

Tungsten has recently been selected as the sole divertor material in ITER [10,11], and is the leading candidate material for DEMO and future fusion reactors. Laboratory experiments performed in linear plasma devices indicate the possibility of substantial surface modification in tungsten exposed to low-energy, helium plasma, or mixed helium–hydrogen plasma, although the observed surface response is strongly temperature-dependent and likely dependent on the ion energy and flux. Pitted surfaces are observed below ≈ 1000 K [12], whereas a "nanostructured," low-density "fuzz" or "coral" surface morphology is observed between approximately 1000 and 2000 K [13-16], while micron-sized holes, or pits, are observed to form above about 2000 K [17-18]. The nanostructured "fuzz" has recently been observed in the divertor regions of a tokamak device operating with a helium plasma as well [19]. Such surface features could lead to changes in heat transfer, fuel (deuterium/tritium) retention [20], increased rates of erosion through both sputtering and dust formation [21], and embrittlement of the divertor, all of which can be detrimental to the plasma [22]. It is important to note that fuzz-like surface modification has not been observed for hydrogen-only plasma exposure, strongly indicating that helium implantation controls this phenomenon. Transmission electron microscopy (TEM) suggests that the nanometer-scale tendrils of the fuzz, and sub-surface regions of tungsten, contain gas bubbles

and/or cavities [23, 24], which implies that bubble evolution is an important process in fuzz formation in tungsten.

Experiments at PISCES-B [25] and NAGDIS-II [26] suggest that the nanostructured fuzz forms when the surface temperature is between 1000 and 2000 K and the incident ion energies are above 22 eV [27]. This raises several questions about the mechanisms that control surface evolution, particularly with respect to the rate of gas bubble formation as a function of temperature and the rate of gas implantation, as well as the mechanisms leading to severe surface roughening. Sharafat and co-workers [28] suggested that near-surface stress gradients cause helium bubbles to be drawn to the surface in the 1000–2400 K temperature range. Krasheninnikov [29] has suggested a viscoelastic model of "fuzz" growth, while Kajita and coworkers [27] found that "pinholes" form on the surface before the "fuzz" begins to grow and suggested that stresses created by bubble formation and growth were responsible for fuzz formation. Alternately, Marynenko and Nagel [30] suggested that adatom formation due to sub-threshold helium impacts, combined with holes from burst bubbles, and subsequent surface diffusion, combined with the trapping (immobilization) of adatoms at the tips of growing islands/fibers are responsible for fuzz formation. Lasa and co-workers have recently used kinetic Monte Carlo simulations to investigate the growth kinetics of a porous, fuzz-like structure [31]. In spite of these efforts, a clear, concise and comprehensive model for fuzz formation, which is experimentally validated, remains to be confirmed.

To summarize, significant challenges exist for modeling plasma surface interactions due to the inherently multiscale nature and complexity of the problem, including a broad span of length and timescales, and the potential for mixed-material formation and evolution that can modify the hydrogen saturation characteristics. At steady state, there are also significant variations in plasma flux between laboratory and tokamak environments, with still-higher implantation fluxes expected in the divertor of ITER and future fusion reactors. This challenge of increasing particle

flux will be further discussed with respect to atomistic simulations and the strong influence of flux on helium gas atom retention and cluster nucleation. Furthermore, ITER and current tokamaks are subject to transient heat and particle flux loads as a result of edge-localized modes (ELMs) as well as plasma containment disruptions that can cause severely high, short-term increases in particle and heat fluxes.

In the remainder of this report, we will first highlight the opportunities presented by a multiscale materials modeling approach using high performance computing to predict PSI behavior in the challenging fusion energy environment. Then, we will discuss recent atomistic modeling that have identified several mechanisms associated with helium clustering beneath tungsten surfaces which provide insight into the formation mechanisms of tungsten nano-fuzz, and then survey areas requiring further study, such as the synergistic helium–hydrogen interactions that will control tritium retention. Finally, the summary will provide a succinct listing of the outstanding issues to be addressed to develop predictive PFC performance models. In addition to the reference citations within this report, there is an attached bibliography in Section VIII, which summarizes the sixteen (16) archival journal articles that resulted from this funding.

III. MULTISCALE MODELING APPROACH

Addressing the critical fusion materials science questions discussed previously requires a number of research activities performed within a computational multiscale materials modeling paradigm [9,32]. The most promising approaches will attack the problem from both a "bottom-up" atomistic-based approach, as well as from a "top-down" continuum perspective that focuses on kinetic models of species reactions and diffusion, as illustrated in Figure 3. Simultaneously attacking such complex and inter-related surface, defect and impurity impingement, diffusion and evolution processes responsible for PFC surface and bulk materials response through both an

atomistic and a continuum approach will minimize the risks of using just a single-scale approach and further the prospects for scale bridging, or multiscale integration.

Such a multiscale approach involves molecular dynamics (MD) as well as binary collision approximation (TRIM) [33] simulations of non-planar, complex geometry surfaces with fractal features [34,35] to describe the fast (i.e., time scale< **O**(10 ns)) dynamic processes of sputtering, re-deposition and surface evolution, as well as bulk defect and helium/hydrogen species evolution in mixed W–He–H–Be systems. Accelerated molecular dynamics (AMD) methods [36-39] can be used to identify key evolution mechanisms occurring on time scales up to seconds. It provides a unique approach that enables deterministic MD simulations of plasma ion flux at appropriate rates, and captures material evolution for durations up to and beyond the time scale of seconds that are needed to identify slower, rare-event processes that contribute to surface, defect and impurity evolution. The AMD approaches, complemented by techniques for activation energy barrier identification, such as the nudged elastic band (NEB) [40, 41] and the dimer [42] method, can determine activation energies and pre-factors that are used to define, within transition-state theory, the reaction rates of individual mechanisms. First-principles density functional theory (DFT) electronic structure methods as implemented in programs such as VASP [43–45], SIESTA [46] or QUANTUM ESPRESSO [47] can be instrumental in providing interaction forces, basic thermodynamic and kinetic interactions and rates, which can be used in fitting interatomic potentials for molecular dynamics simulations, and will be utilized where existing interatomic potentials are deemed inadequate, as is likely the case for the hydrogen – tungsten interactions. Surface evolution phenomena, including re-deposition, fuzz growth and surface migration can be investigated using reduced-parameter continuum techniques

[29] with the goal of developing evolution models that reduce the dynamic complexity to the most pertinent and tractable variables.

Insight into mechanisms and rates of occurrence is the essential outcome of atomic-scale modeling, which can be coupled to reduced parameter models to effectively integrate across the length and time scales in a hierarchical multiscale modeling paradigm. These insights (and corresponding rates) are then used as input in a sequential (hierarchical) fashion to micron to millimeter-scale models; such coarser-scale models may be in the form of either a kinetic Monte Carlo (KMC) simulation or a reaction-diffusion (e.g., the new Xolotl-PSI code [48]) simulation to model the long-time morphological and chemical evolution of a plasma-facing component at, near, and below the surface.

The prevailing approach to couple these multiscale processes is through a hierarchical, information-passing paradigm, as illustrated in Figure 3. The atomistic-based materials modeling approaches naturally link to particle-in-cell, kinetic sheath models, such as VPIC [49] for interfacing across the plasma-surface boundary to provide the incident ion energy and momentum as a function of plasma environment and surface morphology. Continuum models, such as Xolotl-PSI [48] will initially interface with continuum-level fluid models of the plasma scrape-off-layer using SOLPS [50], but could also be linked to a particle-in-cell model to provide a more spatially-dependent description of the incident particle and thermal flux distributions. The bulk material below the surface close to the near-surface region can be modeled using the same set of hierarchical techniques, and a similar approach to scale-bridging can be used. The bulk is where radiation damage processes lead to the nucleation and growth of extended defect clusters,

gas bubbles and local chemical segregation. Therefore, coupling these two spatial zones is important to asses the extent to which these damage processes may mediate, or exacerbate, hydrogen permeation and retention.

The fidelity of the modeling predictions of long-time behavior, whether using continuum approaches or discrete-particle KMC methods, is determined by the extent to which the most important kinetic processes and rates are accurately predicted, and incorporated into the physical reaction-diffusion models. In such a hierarchical modeling approach, independent of the choice of time scale, the use of uncertainty quantification (UQ) techniques can provide important insight for identifying important parameters in process/rate prediction, which result from either the intrinsic error of interatomic potentials used in the atomistic simulations or the inherent uncertainty in environmental conditions in the plasma. The passage of these uncertainties through the multiscale modeling hierarchy will be important in assessing the impact on predicted PFC behavior. Furthermore, the UQ will be used to evaluate the extent to which the coupled 1st- and 2nd-order kinetics influence observed behavior (e.g., how the mobility of a vacancy cluster can influence the resulting size and number density of gas bubbles that act as trapping/retention sites for permeating hydrogen). Such UQ studies of the parameter sensitivities from non-linear coupling amongst the reacting species can prioritize additional atomic-scale simulation studies.

It is important to note that no single model, nor suite of multiscale materials modeling techniques, is currently capable of predicting the performance response of PFC materials to the burning fusion plasma environment. This necessitates a close integration of the modeling activities with a suite of experimental studies, to provide both validation and guidance to the

specific modeling activities, as well as input/output variables. Such interactions increase the likelihood of successfully bridging the scales from the short-time, atomic-scale processes to the longer-term, micron-scale surface morphology changes.

The remainder of this report highlights and reviews results obtained from such a multiscale materials modeling paradigm, and in particular, focus on atomistic MD simulation results that are beginning to elucidate the mechanisms of helium behavior following implantation into tungsten that are likely responsible for the early stages of tungsten surface evolution leading to the nanometer-scale fuzz, as well as have the potential to significantly modify tritium retention behavior. In MD studies, the fidelity of the results depend on the interatomic potentials selected to represent the system, and these potentials are often fit to both electronic structure calculations and experimental data. Commonly available MD programs include LAMMPS [51], or DL-POLY [52], but these codes will not be described here in the interest of brevity. Instead, we focus on a concise description of the corresponding interatomic potentials. For modeling tungsten-helium and tungsten-helium-hydrogen systems, a number of interatomic potential models are readily available. The tungsten-helium system is much simpler to model, since there is little in the way of complex electronic interactions (i.e., chemistry) when modeling a small noble gas such as helium. Tungsten is a body-centered cubic (BCC) material, which has been modeled reasonably successfully using an N-body potential following the Finnis-Sinclair [53] formulation, which is similar to the embedded atom method (EAM) by Daw and Baskes [57]. The original Finnis-Sinclair potential for tungsten has been modified by Ackland and Thetford [54], and subsequently modified at short range by Juslin and Wirth [55]. More recently, Ito and co-workers have fit an EAM-type tungsten potential [56]. It is generally believed that a central

force style potential, such as the EAM or N-body formalism, is sufficient for metallic tungsten and tungsten interactions with noble gas atoms. In terms of the tungsten–helium interaction, Henriksson and co-workers [58], and Juslin and Wirth [55] during this project, have parameterized pairwise, repulsive potentials. For the helium–helium interactions, a potential originally developed by Beck [59], as modified at short distances by Morishita and co-workers [60], is commonly used.

However, it may be more appropriate to model tungsten using a potential that takes into account three-body interactions, such as the Tersoff-type bond order potential [61], especially when considering the possibility of directional bonding of tungsten with hydrogen. Two recent potentials have been fit to describe W-H with a Tersoff-type three-body interaction potential, one by Juslin and co-workers [62] and another by Li and co-workers [63]. As noted in a companion paper in these proceedings [64], the two potentials predict very different hydrogen behavior near tungsten surfaces and in the presence of helium clusters. The energetics of small He-H clusters in bulk tungsten have been determined by the DFT calculations of Becquart and co-workers [65,66], as well as by You and co-workers [67]; and the results of the Juslin potential [60] semi-quantitatively capture the trends exhibited by the binding energies predicted by Becquart and Domain [65]. However, further evaluation of the tungsten–hydrogen–helium interaction potentials and clustering/defect behavior is clearly an area that requires substantial further research using both electronic structure theory modeling, additional experiments, and further fitting of interatomic potentials. The remainder of this article will focus on results obtained in the simpler W-He system, using the Finnis-Sinclair-type potentials.

IV. RESULTS AND DISCUSSION

Numerous groups have recently investigated the effects of low-energy helium implantation below tungsten surfaces using MD simulations, including Lasa, Nordlund and co-workers in Finland [31, 68], Wirth and co-workers in the U.S.A. [69-72], and Ito and co-workers in Japan [56]. While there are some differences in the manner that these different groups have performed the MD simulations, including the interatomic potentials used, the free surface orientations and the temperature and implantation rate; they have each consistently observed similar response associated with helium behavior below tungsten surfaces. When low-energy (<100 eV) helium is injected into tungsten, it has insufficient energy to sputter tungsten or produce atomic displacements in the form of Frenkel pairs. However, it is possible that the helium will create a surface vacancy and tungsten adatom pair. Once the helium comes to rest below the tungsten surface, it becomes an interstitial atom within the BCC tungsten matrix and has very high mobility. The injected helium atom will thus rapidly diffuse in a more-or-less random trajectory that can result in returning to the free surface and escaping, or diffusing deeper into the solid until it encounters a defect or another helium atom. Due to the essentially repulsive nature of the helium – tungsten interactions, combined with the shorter range and lower magnitude of repulsive helium-helium interactions, the helium has a strong driving force to cluster (in order to minimize the number of repulsive tungsten-helium interactions). Small helium clusters are themselves mobile, as long as all of the helium reside in interstitial positions in the BCC tungsten lattice, and any clusters that form continue to perform an essentially random walk with fast diffusivity (activation energies for interstitial helium and helium cluster migration range from about 0.15 to 0.45 eV using these interatomic potentials [73]). As the migrating helium clusters grow larger, they eventually reach a condition in which the effective pressure generated is

sufficient to create a tungsten vacancy and self-interstitial (Frenkel) pair, in a process called trap mutation [68-72]. The size at which trap mutation first occurs depends on a number of factors, including the temperature and the proximity of the helium cluster to the free surface, as well as the surface's crystallographic orientation [71,72]. When trap mutation occurs, the high-pressure interstitial helium cluster situates itself on/near the newly created vacancy, and the cluster essentially becomes immobile since it requires either additional vacancies or interstitial-vacancy recombination and kick-out mechanisms to again become mobile. The resulting helium-vacancy cluster containing multiple helium atoms then serves as a nucleus for helium gas bubbles at higher fluence, through the absorption of mobile helium interstitial atoms and helium clusters during continued gas implantation. As the high-pressure gas bubbles continue to grow and the pressure in the bubbles continues to rise due to the absorption of additional helium, eventually this pressure reaches the level required for dislocation loop punching [56, 68-70]. The punching of prismatic dislocation loops allows the volume of the gas bubbles to increase through absorbing a prismatic platelet or facet of vacant lattice sites and thereby reducing their pressure. The fate of the tungsten interstitial atoms produced by either trap mutation or dislocation loop punching is strongly influenced by the presence of a nearby free surface, leading to significant roughening of the tungsten surface through the formation of individual tungsten adatoms as single self-interstitials annihilate at the surface, and formation of coherent islands of tungsten atoms formed by way of annihilation of prismatic loops. The final process observed in MD simulations is the rupture of over-pressurized helium gas bubbles located near the surface [56, 68-70]. Ito [56] and Sefta [70] have mapped out the conditions associated with the rupturing of spherical [56,70] or lenticular [70] gas bubbles below the surface, in terms of gas pressure [70] or helium to vacancy ratio [56].

The mechanisms just described are evident in Figure 4, which shows results from an MD simulation of helium implantation below a (100) tungsten surface intersected by a Σ5 grain boundary, using the tungsten N-body potential and tungsten-helium pair potential developed by Juslin and Wirth [55]. The simulation cell was approximately 6.4 nm in the x and y directions, for which periodic boundary conditions were used, and approximately 10 nm in the z-direction along [100], where the simulation cell was bounded by a free surface intersected by a Σ5 grain boundary. For the results of Fig. 4, the temperature was 2000 K, and throughout the simulation, thermalized helium atoms were introduced at random locations below the surface at a distance determined from the cumulative helium depth distribution corresponding to tungsten exposure to 60 eV He at a rate of about $5x10^{27}$ He/(m^2-s). The results, with increasing helium exposure from about 0.9 to $1.1x10^{20}$ He/m^2, clearly indicate the formation and evolution of sub-surface helium gas bubbles as well as some degree of surface roughening. The key mechanistic observation in this (and other) MD simulations are that small helium clusters form rapidly and are highly mobile until reaching a size of seven to eight helium atoms. At that size, the helium atom clusters undergo a 'trap mutation' process in which the excess gas pressure creates a Frenkel pair of a single tungsten self-interstitial atom and a tungsten vacancy. The helium cluster then expands to fill the vacant lattice sire, releasing the built-up pressure. At short times, the self-interstitial atoms stay bound in the vicinity of the over-pressurized gas bubbles, until a sufficient self-interstitial atom density is reached, at which point the self-interstitials spontaneously organize into prismatic dislocation loops that migrate to the surface and annihilate as adatom islands. The continued introduction of helium into the system drives further growth of over-pressurized bubbles that presumably continue to expand through trap mutation processes, undergo bubble

coalescence into dense, pressurized networks, and eventually can burst or rupture through to the surface. Bubble rupture both releases the entrapped helium and causes significant additional surface roughening through the cratering process of the tungsten atoms in the ruptured ligament above the bubble [68,60].

Of course, the results shown in Fig. 4 are strongly influenced by the very fast rate of introducing helium below the tungsten surface, which is approximately 10^5 times faster than in linear plasma devices such as PISCES-B [25] or NAGDIS-II [26]. Another factor in the simulations that is beginning to be recognized as influencing at least the early stage evolution of tungsten surface roughness prior to the formation of fuzz, is the surface orientation. Indeed, Parish and co-workers [74] have shown experimentally that the surface roughness feature shape depends on the tungsten surface normal following exposure to 80 eV helium ions at 1130°C and to a fluence of $4x10^{24}$ Hem^{-2} and an implantation flux of about 10^{20} $Hem^{-2}s^{-1}$. However, once the nanometer-scale fuzz forms, there is no longer any observed dependence of initial surface orientation, grain size, or even solute or oxide particle additions, as shown by Baldwin and Doerner [75]. Thus, while surface orientation is an important consideration in the early tungsten surface and sub-surface bubble evolution, it is also clear that the helium implantation rate is an important parameter. It should be noted that the vast majority of MD simulations in the literature [56, 68-70] have used implantation rates that are many orders of magnitude higher than current linear devices or expected in the ITER divertor. Since helium can strongly self-trap itself, the effect of this much higher implantation rate is not likely to alter the key mechanisms observed in the MD simulations discussed previously, but it can be expected to quantitatively modify the amount of helium retained within the specimen, as well as the number density and size evolution (growth rate) of helium bubbles that drives the rate of dislocation loop punching and bubble bursting.

Figure 5 shows the percentage of helium retained as a function of tungsten surface orientation and the implantation flux, as observed in MD simulations. Here retention is meant to indicate the percentage of helium atoms that remain below the tungsten surface, either in the form of a single interstitial helium atoms, or trapped helium clusters and bubbles. As such, retention is always near 100% at the lowest fluences, but then decreases as the helium is able to diffuse back to the surface. There is a marked difference in the fraction of helium retained between {001} or {011} surfaces as compared to the {111} or {211} surfaces at comparable flux and fluence conditions. This suggests that a mechanism exists to prevent helium from diffusing to the surface and/or escaping from the surface in the {111} and {211} cases. Indeed, Hu and co-workers [71,72], and Hammond and Wirth [76], have shown that the size of a helium cluster for which trap mutation is likely to occur is strongly dependent on the proximity to a free surface, as well as on surface orientation. Figure 5 also shows the rather strong effect of implantation flux on helium retention, for example, the amount of retention below a (001) surface at an implantation flux of ~2.5×10^{27} $Hem^{-2}s^{-1}$ is between 60 and 70%, whereas it is reduced to about 30% with a flux reduced by about 100 times. In addition, some of the MD simulations shown in Figure 5 include either a $\Sigma 3$ or $\Sigma 5$ grain boundary that is oriented perpendicular to the free surface. The presence of such boundaries is observed to increase the amount of retained helium by about 5-10% over the corresponding simulation in an otherwise initially perfect tungsten slab, which results from the additional helium trapping sites within the grain boundaries that serve as helium cluster and bubble nucleation sites. The effect of helium implantation rate remains an important issue in determining and experimentally validating the number density and size of sub-surface helium bubbles prior to the onset of fuzz formation in tungsten exposed to low-energy helium plasma implantation.

Another important topic for future research is that of the helium-hydrogen synergy, and its potential impact on tritium retention in the ITER tungsten divertor. Figure 6 summarizes available experimental observations of the complex synergy between helium and deuterium with respect to plasma-surface interactions, as summarized from Miyamoto and collaborators [24], along with some atomistic modeling results from Juslin and Wirth [77]. In these experiments, a linear plasma device was used to expose tungsten at 200°C to either a pure deuterium or mixed deuterium (D) – helium (He) plasma with a negative bias potential of 60 or 120 eV and an ion flux of about 10^{22} $m^{-2}s^{-1}$. Figure 6a shows a transmission electron microscopy (TEM) image of the sub-surface structure of the tungsten exposed to the mixed D-He plasma with energy of ~60eV and a gas implantation fluence of about $5x10^{25}$ m^{-2} (~$5x10^{3}$ s), clearly identifying the formation of gas bubbles within a depth of about 20 nm near the surface [24]. Miyamoto [24] estimated that the bubbles had an average size of 1.8 nm. Figure 6b shows the surface evolution of the tungsten following exposure to either pure deuterium or mixed deuterium-helium plasma at 200°C with an incident ion energy of ~120 eV and a gas implantation fluence of about $5x10^{25}$ m^{-2} (~$5x10^{3}$ s), along with the results of deuterium thermal desorption spectroscopy. The results in Fig. 6b clearly indicate that the presence of helium in the plasma reduces the occurrence of surface blistering (from SEM images) and also modifies the deuterium retention behavior, as much less deuterium is released from the sample during thermal annealing up to 1300K (approximately 1/3 of the tungsten melting temperature), and this could imply that more deuterium maybe retained within the specimen. Figures 6c and 6d show results from atomistic simulations to evaluate the partitioning of hydrogen in the vicinity of a helium gas bubble with a radius of 2 nm, and for varying amounts of initial hydrogen concentration [77]. Figure 6c clearly shows that hydrogen is attracted to the gas bubble, where it predominately partitions to the periphery of the bubble, along with some partitioning of hydrogen into the tungsten matrix next to the bubble. Indeed, Fig. 6d quantitatively plots the relative distribution of hydrogen observed following the MD simulation at 900K, where the initial uniform hydrogen distribution within the bubble partially diffuses into the matrix to become localized near the bubble-matrix surface.

These results indicate significant hydrogen (i.e., titium and deuterium) trapping at the bubble, and are consistent with recent electronic structure calculations of hydrogen-helium synergies in tungsten [66], but only begin to elucidate the necessary calculations required in order to quantify the expected tritium retention in the ITER tungsten divertor. Likewise, these experimental results show a clear synergy between hydrogen and helium in affecting surface morphology, sub-surface gas bubble formation and deuterium/tritium retention [66,77]. However, these experiments have not been conducted at the conditions expected in ITER, which will involve steady temperatures in the range of 400 to 800°C and D/T/He ion energies in the range of 10 to 100 eV at fluxes on the order of 10^{24} $m^{-2}s^{-1}$.

V. SUMMARY AND FUTURE WORK

The performance of plasma facing components (PFC) is critical for ITER and future magnetic fusion reactors. The ITER divertor will consist of tungsten, which is the primary candidate for future reactors. This article has reviewed the numerous and significant challenges associated with plasma-surface interactions that relate to the inherently multiscale nature and complexity of the problem, which involves a large span of length and timescales, the potential for mixed-material (e.g., W-Be and W-C) formation and evolution that can modify the hydrogen saturation characteristics, and significant differences in plasma flux between laboratory and tokamak environments and atomistic modeling studies.

We have also highlighted a multiscale materials modeling paradigm that can utilize high-performance computing to develop predictive models of PFC performance, before reviewing recent results from atomistic MD simulations that have identified a number of important mechanisms controlling the behavior of helium implanted into tungsten. These simulations reveal these the following sequence of events, or important mechanisms: (1) embedding of helium atoms below the surface; (2) their diffusion either back to the surface or deeper where

other helium atoms or crystalline defects can be encountered, resulting in clustering due to strongerW–He repulsions compared to He–He repulsions; (3) so-called “trap mutation” of (mobile) helium clusters to form tungsten self-interstitials and (immobile) helium-vacancy clusters/bubbles; (4) agglomeration of self-interstitials into prismatic loops through the dislocation loop punching process of over-pressurized gas bubbles; and (5) the glide of such dislocations to the surface or another tungsten “sink”. Finally, another mechanism involves the bursting of over-pressurized gas bubbles that are close to the tungsten surface. The net effect of these processes is to roughen the tungsten surface through the creation of coherent “islands” of tungsten atoms accompanied by bubbles near the surface or voids/craters that result from ruptured bubbles. While numerous researchers have observed these mechanisms, it is clear that the helium implantation rate will influence both the amount of retained helium and the rate of surface roughness, and at present, no unified and experimentally consistent model exists to explain the formation of tungsten nanofuzz.

Among the most pressing future needs within the field are the continued evaluation of the effect of implantation rate and surface temperature on the surface morphological response of tungsten exposed to low-energy plasma bombardment, and the analysis of synergistic interactions between helium and hydrogen that are expected to influence the amount of tritium retention and fuel (hydrogen isotope) saturation in the tungsten divertor of ITER. This requires a number of research activities across a broad range of length scales, as well as specific experiments to test our understanding of hydrogen – tungsten – helium interactions on tungsten surfaces.

VI. ACKNOWLEDGEMENTS

Support for this work was provided through the Plasma-Surface Interactions Science Center, funded by the U. S. Department of Energy, Office of Fusion Energy Sciences under award number DE–SC00–02060. Partial support for this work was also provided through the Scientific Discovery through Advanced Computing (SciDAC) program on Plasma Surface Interactions, funded by U. S. Department of Energy, Office of Science, Advanced Scientific Computing Research and Fusion Energy Sciences under award number DE-SC00–08875.

This research used resources of the National Energy Research Scientific Computing Center (NERSC) at Lawrence Berkeley National Laboratory and the Argonne Leadership Computing Facility (ALCF) at Argonne National Laboratory, which are supported by the Office of Science of the U.S. Department of Energy under contracts DE–AC02–06CH11231 and DE–AC02–06CH11357, respectively.

Oak Ridge National Laboratory is managed by UT-Battelle, LLC for the U. S. Department of Energy under contract DE–AC05–00OR22725.

VII. REFERENCES

[1] Introduction to the Grand Challenges for Engineering, http://www.engineeringchallenges.org/cms/8996/9221.aspx, 2008.
[2]. G.M. McCracken, *Journal of Nuclear Materials* **63** (1976) 91.
[3]. D.E. Post and R. Behrisch, editors, Physics of plasma-wall interactions in controlled fusion, Basic Books, 1986.
[4]. G.M. McCracken, editor, Plasma surface interactions in controlled fusion devices, Elsevier Science Ltd, 1978.
[5]. R.R. Hasiguti, editor, First International Conference on Fusion Reactor Materials, North-Holland, 1985.
[6]. R. A. Johnson, Physics of Radiation Effects in Crystals, Modern Problems in Condensed Matter Sciences, Elsevier, Amsterdam, 1986.
[7]. G. Federici, C.H. Skinner, J.N. Brooks, J.P. Coad, C. Grisolia, A.A. Haasz, A. Hassanein, V. Philipps,C.S. Pitcher, J. Roth, and W.R. Wampler adn D.G. Whyte, *Nuclear Fusion* **41** (2001).
[8]. A.R. Raffray, R. Nygren, D.G. Whyte, S. Abdel-Khalik, R. Doerner, F. Escourbiac, T. Evans, R.J. Goldston, D.T. Hoelzer, S. Konishi, P. Lorenzetto, M. Merola, R. Neu, P. Norajitra, R.A. Pitts, M. Rieth,M. Roedig, T. Rognlien, S. Suzuki, M.S. Tillack, and C. Wong, *Fusion Engineering and Design* 85, 93 (2010).
[9]. B.D. Wirth, K. Nordlund, D.G. Whyte, and D. Xu, Fusion materials modeling: challenges and opportunities, *MRS Bulletin* 36, 216.
[10]. R.A. Pitts, S. Carpentier, F. Escourbiac, T. Hirai, V. Komarov, S. Lisgo, A.S. Kukushkin, A. Loarte, M. Merola, A. Sashala Naik, R. Mitteau, M. Sugihara, B. Bazylev, and P.C. Stangeby, *Journal of Nuclear Materials* **438** (2013) S48-S56.
[11]. https://www.iter.org/mach/divertor
[12]. Iwakiri H, Yasunaga K, Morishita K, Yoshida N 2000 *J. Nucl. Mater.* **283–287** 1134–1138.
[13] Takamura S, Ohno N, Nishijima D, Kajita S 2006 *Plasma Fusion Res.* **1** 051.

[14] Baldwin M J, Doerner R. P. 2008 *Nucl. Fusion* **48** 035001.
[15] Baldwin M J, Doerner R P, Nishijima D, Tokunaga K, Ueda Y 2009 *J. Nucl. Mater.* **390–391** 886–890.
[16] Zenobia S J, Kulcinski G L 2009 *Phys. Scr.* **T138** 014049.
[17] Nishijima D, Ye M-Y, Ohno N, Takamura S 2004 *J. Nucl. Mater.* **329–333** 1029–1033.
[18] Nishijima D, Miyamoto M, Iwakiri H, Ye M-Y, Ohno N, Tokunaga K, Yoshida N, Takamura S 2005 *Mater. Trans.* **46** 561–564.
[19] Wright G M, Brunner D, Baldwin M J, Doerner R P, Labombard B, Lipschultz B, Terry J L, Whyte D G 2012 *Nucl. Fusion* **52** 042003.
[20] Baldwin M J, Doerner R P, Wampler W R, Nishijima D, Lynch T, Miyamoto M 2011 *Nucl. Fusion* **51** 119501.
[21] Umstadter K R, Doerner R, Tynan G 2009 *Phys. Scr.* **T138** 014047.
[22] Hill K W, Bitter M, Eames D, von Goeler S, Goldman M, Sauthoff N R, Silver E 1982 *Low Energy X-Ray Emission from Magnetic Fusion Plasmas*, Princeton University Technical Report PPPL–1807 (Princeton University, Princeton, New Jersey).
[23] Kajita S, Takamura S, Ohno N, Nishijima D, Iwakiri H, Yoshida N 2007 *Nucl. Fusion* **47** 1358–1366.
[24]. M. Miyamoto, D. Nishijima, M.J. Baldwin, R.P. Doerner, Y. Ueda, K. Yasunaga, N. Yoshida, and K. Ono, *Journal of Nuclear Materials* **415** (2011) S657-S660.
[25] Hirooka Y, Conn R W, Sketchley T, Leung W K, Chevalier G, Doerner R, Elverum J, Goebel D M, Gunner G, Khandagle M, Labombard B Lehmer R, Luong P, Ra Y, Schmitz L, Tynan G 1990 *J. Vac. Sci. Technol. A.* **8** 1790–1797.
[26] Ezumi N, Ohno N, Uesugi Y, Park J, Watanabe S, Cohen S A, Krasheninnikov S I, Pigarov Y A, Takagi M, Takamura S 1997 In *Proceedings of the 24th European Physical Society Conference on Controlled Fusion and Plasma Physics, Berchtesgaden* (Max Plank Institute für Plasma Physik: Garching) Vol. 21A, p 1225
[27]. Kajita S, Sakaguchi W, Ohno N, Yoshida N, Saeki T 2009 *Nucl. Fusion* **49** 095005.
[28] Sharafat S, Takahashi A, Nagasawa K, Ghoniem N 2009 *J. Nucl. Mater.* **389** 203–212.
[29]. Krasheninnikov S I 2011 *Phys. Scr.* **T145** 014040.
[30]. Martynenko and Nagel, *Plasma Physics Reports* **38** (2012) 996.
[31]. A. Lasa, S.K. Tahtinen and K. Nordlund, *EPL* **105** (2014) 25002.
[32]. B. D. Wirth, G. R. Odette, J. Marian, L. Ventelon, J. A. Young, and L. A. Zepeda-Ruiz, *Journal of Nuclear Materials* **329–333**, 103 (2004).
[33]. James F. Ziegler, editor, The Stopping and Range of Ions in Solids, volume 1 of The Stopping and Ranges of Ions in Matter, Pergamon Press, New York, 1985.
[34] D. N. Ruzic and H. K. Chiu, *Journal of Nuclear Materials* **162–164**, 904 (1989).
[35] D. N. Ruzic, *Nuclear Instruments and Methods B* **47**, 118 (1990).
[36]. A.F. Voter, *J. Chem. Phys.* **106**, 4665 (1997).
[37] A.F. Voter*, Phys. Rev. B* **57**, R13985 (1998).
[38] M.R. Sørensen and A.F. Voter*, J. Chem. Phys.* **112**, 9599 (2000).
[39] A.F. Voter, F. Montalenti, and T.C. Germann, *Annu. Rev. Mater. Res.* **32,** 321 (2002).
[40]. Hannes Jónsson, Greg Mills, and Karsten W. Jacobsen, Nudged Elastic Band Method for Finding Minimum Energy Paths of Transitions, in B. J. Berne, G. Ciccotti, and D. F. Coker, editors, Classical and Quantum Dynamics in Condensed Phase Simulations, chapter 16, pages 385–405, World Scientific, 1998.
[41] Graeme Henkelman, Blas P. Uberuaga, and Hannes Jónsson, *Journal of Chemical Physics* **113**, 9901 (2000).
[42] J. Kästner and P. Sherwood, *Journal of Chemical Physics* **128**, 014106 (2008).
[43] G. Kresse and J. Hafner, *Physical Review B: Condensed Matter and Materials Physics* **47**, 558 (1993).

[44] G. Kresse and J. Hafner, *Physical Review B: Condensed Matter and Materials Physics* **49**, 14251 (1994).
[45] G. Kresse and J. Furthmüller, *Computational Materials Science* **6**, 15 (1996).
[46]. http://departments.icmab.es/leem/siesta/
[47]. http://www.quantum-espresso.org/
[48]. http://sourceforge.net/projects/xolotl-psi/
[49]. K. J. Bowers, B. J. Albright, L. Yin, B. Bergen, and T. J. T. Kwan, *Phys. Plasmas* **15**, 055703 (2008).
[50] R. Schneider, X. Bonnin, K. Borrass, D. P. Coster, H. Kastelewicz, D. Reiter, V. A. Rozhansky, and B. J. Braams, *Contributions to Plasma Physics* **46**, 3 (2006).
[51]. http://lammps.sandia.gov
[52]. http://www.csar.cfs.ac.uk/user_information/software/chemistry/dl_poly.shtml
[53]. Finnis M W, Sinclair J E 1984 *Philos. Mag. A* **50** 45–55
[54]. Ackland G J, Thetford R, 1987 *Philos. Mag. A* **56** 15–30
[55] Juslin N, Wirth B D 2013 *J. Nucl. Mater.* **432** 61–66
[56]. A.M. Ito, Y. Yoshimoto, S. Saito, A. Takayama, and H. Nakamura, *Phys. Scr.* **T159** (2014) 014062.
[57]. S.M. Daw and M.I. Baskes, *Phys. Rev. Lett.* **59** (1983) 1285.
[58]. K.O.E. Henriksson, K. Nordlund, J. Keinonen, S. Sundholm, and M. Patzschke, *Phys. Scr.* **T108** (2004) 95.
[59]. Beck D E 1986 Mol. Phys. **14** 311–315; **15** 332
[60]. Morishita K, Sugano R, Wirth B D, Diaz de la Rubia T 2003 *Nucl. Instrum. Meth. Phys. Res. B* **202** 76–81
[61]. J. Tersoff, Phys. Rev. B 37 (1988) 6991–7000.
[62]. N. Juslin, P. Erhart, P. Träskelin, J. Nord, K.O.E. Henriksson, K. Nordlund, E. Salonen, K. Albe, J. Appl. Phys. 98 (2005) 123520.
[63]. X.-C. Li, X. Shu, Y.-N. Liu, F. Gao, G.-H. Lu, J. Nucl. Mater. 408 (2011) 12–17.
[64]. M.A. Cusentino, K.D. Hammond, F. Sefta, N. Juslin, and B.D. Wirth, manuscript P1-011 "A Comparison of Interatomic Potentials for Modeling Tungsten-Hydrogen-Helium Plasma-Surface Interactions", *Journal of Nuclear Materials* (2014) this volume, accepted.
[65]. C.S. Becquart and C. Domain, *Journal of Nuclear Materials* **386-388** (2009) 109-111.
[66]. G.-H. Lu, H.-B. Zhou and C.S. Becquart, *Nuclear Fusion* **54** (2014) 086001.
[67]. Y.-W. You, D. Li, X.-S. Kong, X. Wu, C.S. Liu, Q.F. Fang, B.C. Pan, J.L. Chen, and G.-N. Luo, *Nuclear Fusion* **54** (2014) 103007.
[68]. A. Lasa, K.O.E. Henriksson, and K. Nordlund, *Nuclear Instruments and Methods B* **303** (2013) 156.
[69]. F. Sefta, K.D. Hammond, N. Juslin and B.D. Wirth, *Nuclear Fusion* **53** (2013) 073015.
[70]. F. Sefta, N. Juslin and B.D. Wirth, *Journal of Applied Physics* **113** (2013) 243518
[71]. L. Hu, K.D. Hammond, B.D. Wirth, and D. Maroudas, *Journal of Applied Physics* **115** (2014) 173512
[72]. L. Hu, K.D. Hammond, B.D. Wirth and D. Maroudas, *Surface Science* **626** (2014) 21-25.
[73]. D. Perez, T. Vogel and B.P. Uberuaga, *Physical Review B* ***90*** (2014) 014102.
[74]. C.M. Parish, H. Hijazi, H.M. Meyer, and F.W. Meyer, *Acta Materialia* **62** (2014) 173-181.
[75]. M.J. Baldwin and R. P. Doerner, *J. Nucl. Materials* **404** (2010) 165.
[76]. K.D. Hammond and B.D. Wirth, *Journal of Applied Physics* **116** (2014) 143301.
[77]. N. Juslin and B.D. Wirth, "*Journal of Nuclear Materials* **438** (2013) 1221-1223

VIII. BIBLIOGRAPHY OF ARCHIVAL PUBLICATIONS RESULTING FROM THIS FUNDING

Refereed Journal Publications (15):

N. Juslin and B.D. Wirth, "Interatomic potentials for simulation of He bubble formation in W", *Journal of Nuclear Materials* **432** *(*2013) 61-66.

F. Sefta, N. Juslin, K.D. Hammond, and B.D. Wirth, "Molecular dynamics simulations of the effect of sub-surface helium bubbles on the sputtering yield of tungsten", *Journal of Nuclear Materials* **438** *(2013)* 493-496.

N. Juslin and B.D. Wirth, "Molecular dynamics simulation of the effect of sub-surface helium bubbles on hydrogen retention in tungsten", *Journal of Nuclear Materials* **438** *(2013)* 1221-1223.

F. Sefta, K.D. Hammond, N. Juslin and B.D. Wirth, "Tungsten Surface Evolution by Helium Bubble Nucleation, Growth and Rupture", *Nuclear Fusion* **53** (2013) 073015.

F. Sefta, N. Juslin and B.D. Wirth, "Helium bubble bursting in tungsten", *Journal of Applied Physics* **113** (2013) 243518 (9 pages)

L. Hu, K.D. Hammond, B.D. Wirth, and D. Maroudas, "Interactions of mobile helium clusters with surfaces and grain boundaries of plasma-exposed tungsten", *Journal of Applied Physics* **115** (2014) 173512 (8 pages)

S.I. Krasheninnikov, T. Faney, and B.D. Wirth, "On helium cluster dynamics in tungsten plasma facing components of fusion devices", *Nuclear Fusion* **54** (2014) 073019 (12 pages).

L. Hu, K.D. Hammond, B.D. Wirth and D. Maroudas, " Dynamics of Small Mobile Helium Clusters Near Tungsten Surfaces", *Surface Science* **626** (2014) 21-25. (August 2014)

T. Faney and B.D. Wirth, "Spatially-dependent cluster dynamics modeling of microstructure evolution in low energy helium irradiated tungsten", *Modeling and Simulation in Materials Science & Engineering,* **22** (2014) 065010 (17 pages) (Sept2014).

K.D. Hammond and B.D. Wirth, "Crystal orientation effects on helium ion depth distributions and adatom formation processes in plasma-facing tungsten", *Journal of Applied Physics* **116** (2014) 143301(8 pages)

T. Faney, S.I. Krasheninnikov and B.D. Wirth, "Spatially dependent cluster dynamics model of He plasma surface interaction in tungsten for fusion relevant conditions", *Nuclear Fusion* **55** (2015) 013014.

F. Ferroni, K.D. Hammond and B.D. Wirth, Sputtering Yields of Pure and Helium-Implanted Tungsten under Fusion-Relevant Conditions Calculated using Molecular dynamics, *Journal of Nuclear Materials* (2015) in press, http://dx.doi.org/doi:10.1016/j.jnucmat.2014.12.090.

M.A. Cusentino, K.D. Hammond, F. Sefta, N. Juslin, and B.D. Wirth, "A Comparison of Interatomic Potentials for Modeling Tungsten-Hydrogen-Helium Plasma-Surface Interactions", *Journal of Nuclear Materials* (2015) in press, http://dx.doi.org/doi:10.1016/j.jnucmat.2014.10.043.

R. D. Kolasinski, K.D. Hammond, J.A. Whaley, D.A. Buchenauer, and B.D. Wirth, "Analysis of hydrogen adsorption and surface binding configuration on tungsten using direct recoil spectrometry", *Journal of Nuclear Materials* (2015) in press, http://dx.doi.org/doi:10.1016/j.jnucmat.2014.11.115.

BD Wirth, K.D. Hammond, S.I. Krashenninikov, and D. Maroudas, "Challenges and Opportunities of Modeling Plasma Surface Interactions in Tungsten using High Performance Computing, *Journal of Nuclear Materials* (2015) in press, http://dx.doi.org/doi:10.1016/j.jnucmat.2014.11.072

Invited Articles in Archival Magazines, Journals or Book Chapters (1):

B.D. Wirth, K. Nordlund, D.G. Whyte, and D. Xu, "Fusion materials modeling: Challenges and opportunities", *Materials Research Society Bulletin* **36** (2011) 216-222.

IX. FIGURES

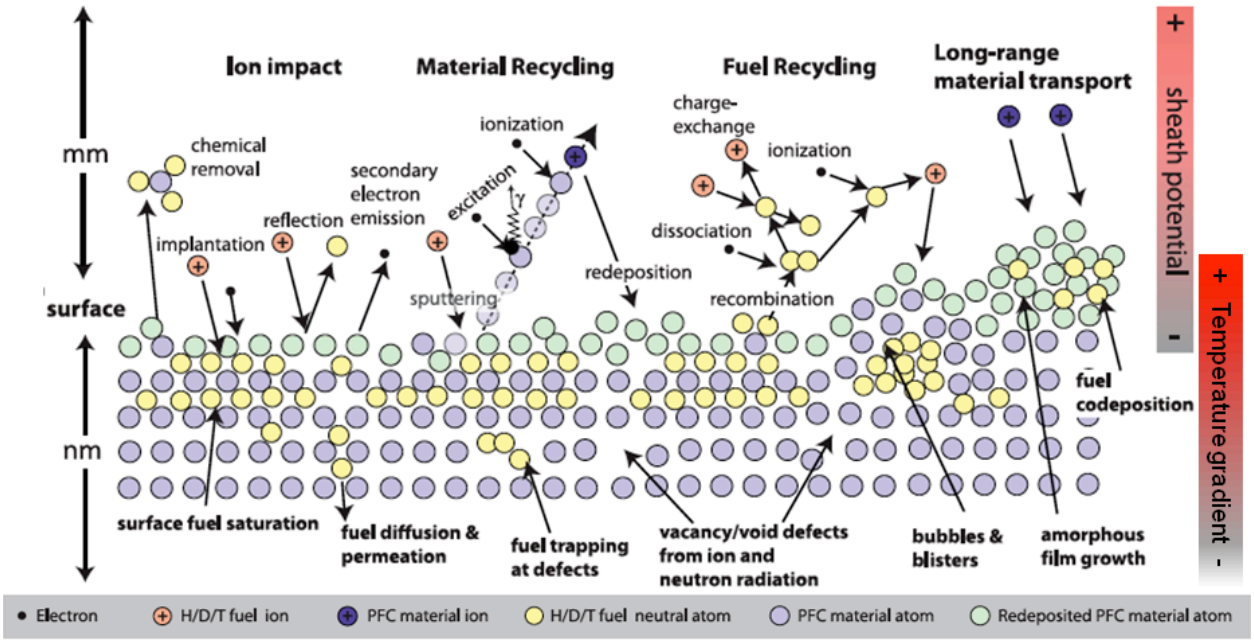

Figure 1. *Schematic illustration of the synergistic plasma surface interaction processes that dictate material evolution and performance in the magnetic fusion plasma environment, as reproduced from [9].*

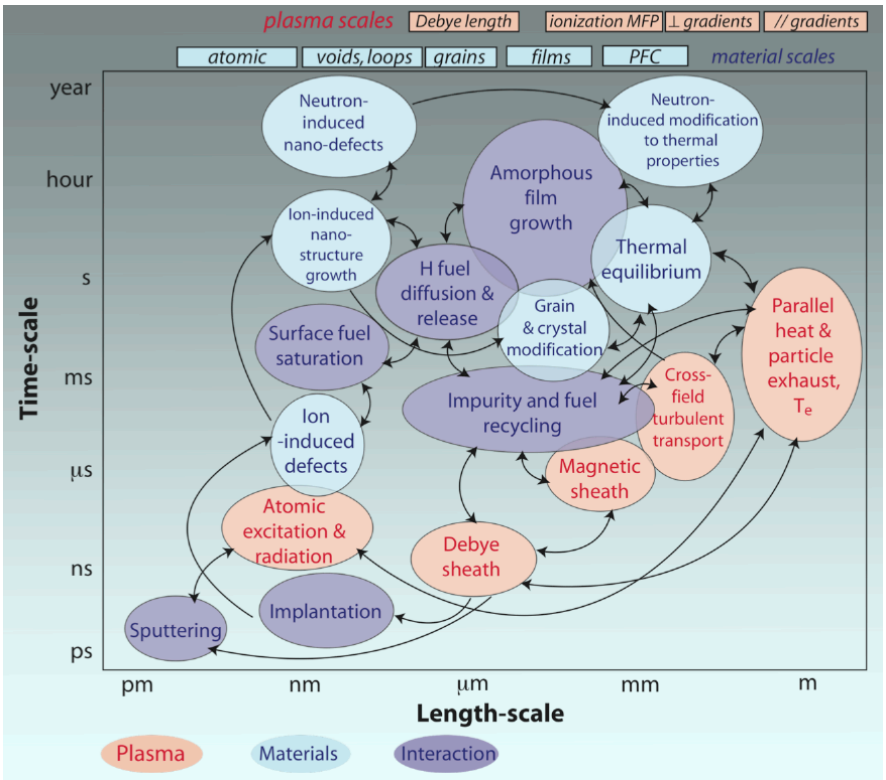

Figure 2. *Graphical representation of the multiple time and length-scales involved in the inherently coupled processes and phenomena which dictate plasma materials interactions in the boundary plasma region of magnetic fusion devices. Processes occurring within the plasma are denoted in light red, while those in the near-surface and bulk materials are in light blue, and the important plasma – materials interactions are identified in light purple, as reproduced from [9].*

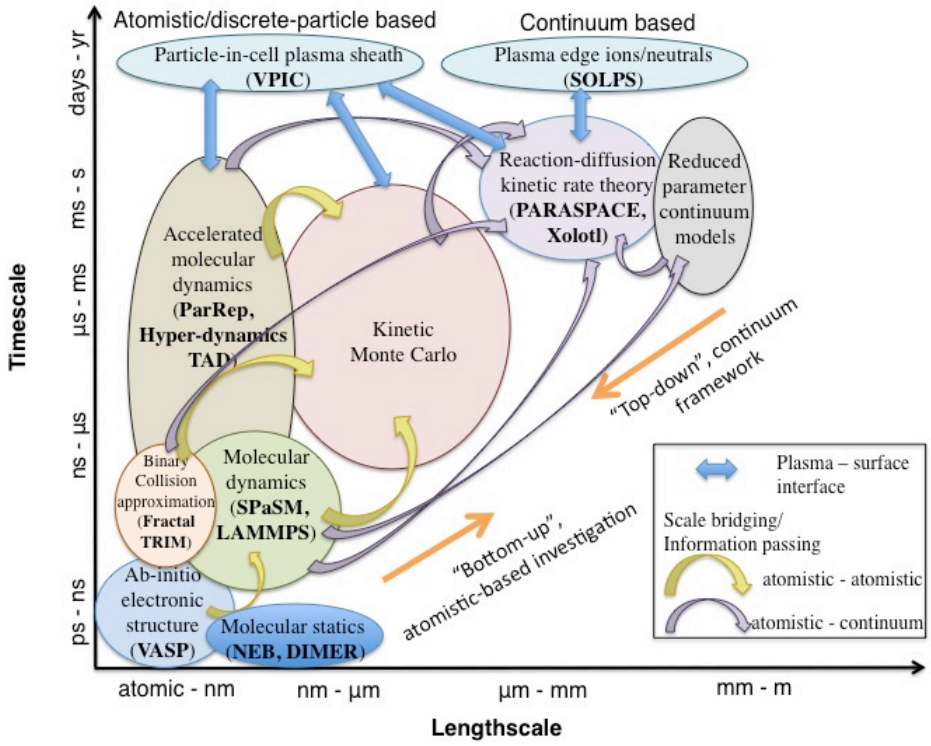

Figure 3: *Illustration of a multiscale modeling approach for plasma-surface interactions, including discrete particle and continuum-scale techniques for scale-bridging across the multitude of processes occurring on disparate time and length scales that control PFC behavior.*

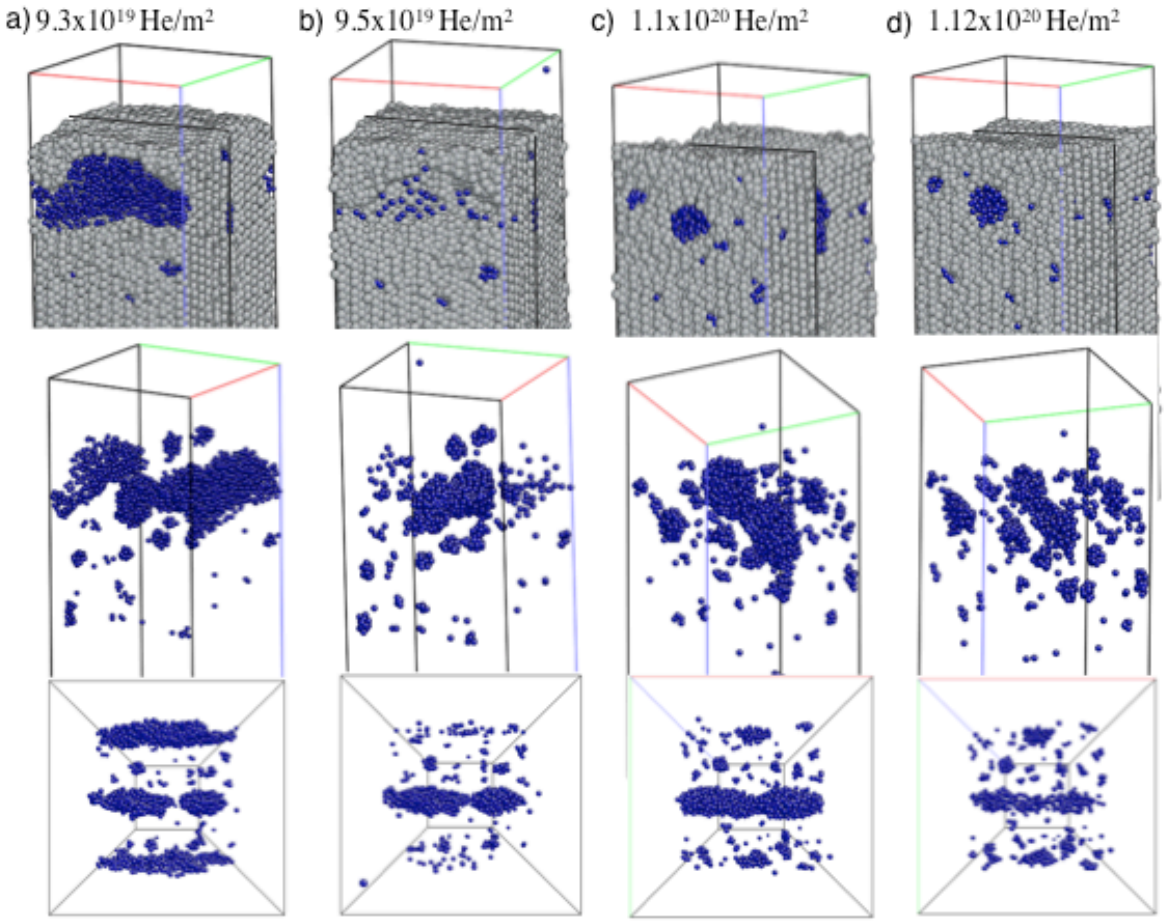

Figure 4: *Visualization of MD simulations of tungsten (gray spheres) exposed to a 60 eV helium plasma implantation (blue spheres are helium atoms), which shows the accumulation of surface roughness near a Σ5 grain boundary that intersects a (100) free surface and the helium gas bubble distributions beneath the surface as a function of increasing implanted helium dose. The sub-surface helium bubble populations are viewed from an angle (middle of Figure) and from a top-down perspective (bottom), with the tungsten atoms removed for ease of visualization.*

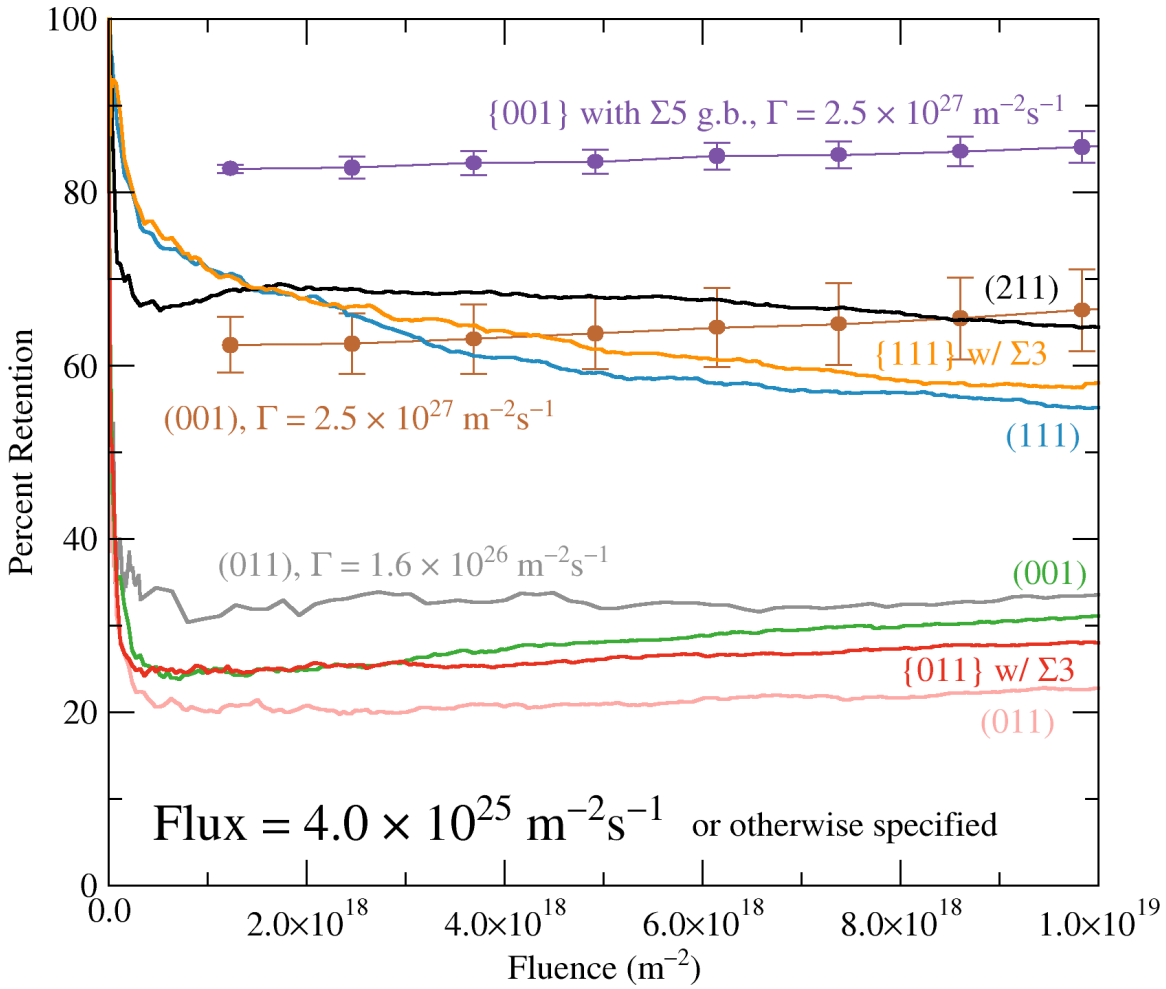

Figure 5: *Percentage of implanted helium that is retained within an MD simulation cell as a function of fluence for various surface orientations (i.e., with {001}, {110}, {211}, or {111} surfaces) with initially perfect single crystals, or otherwise-perfect crystals containing grain boundaries that intersect the free surface, and for several implantation fluxes. Fluxes and fluences shown exclude reflected ions, as described by Hammond and Wirth [76].*

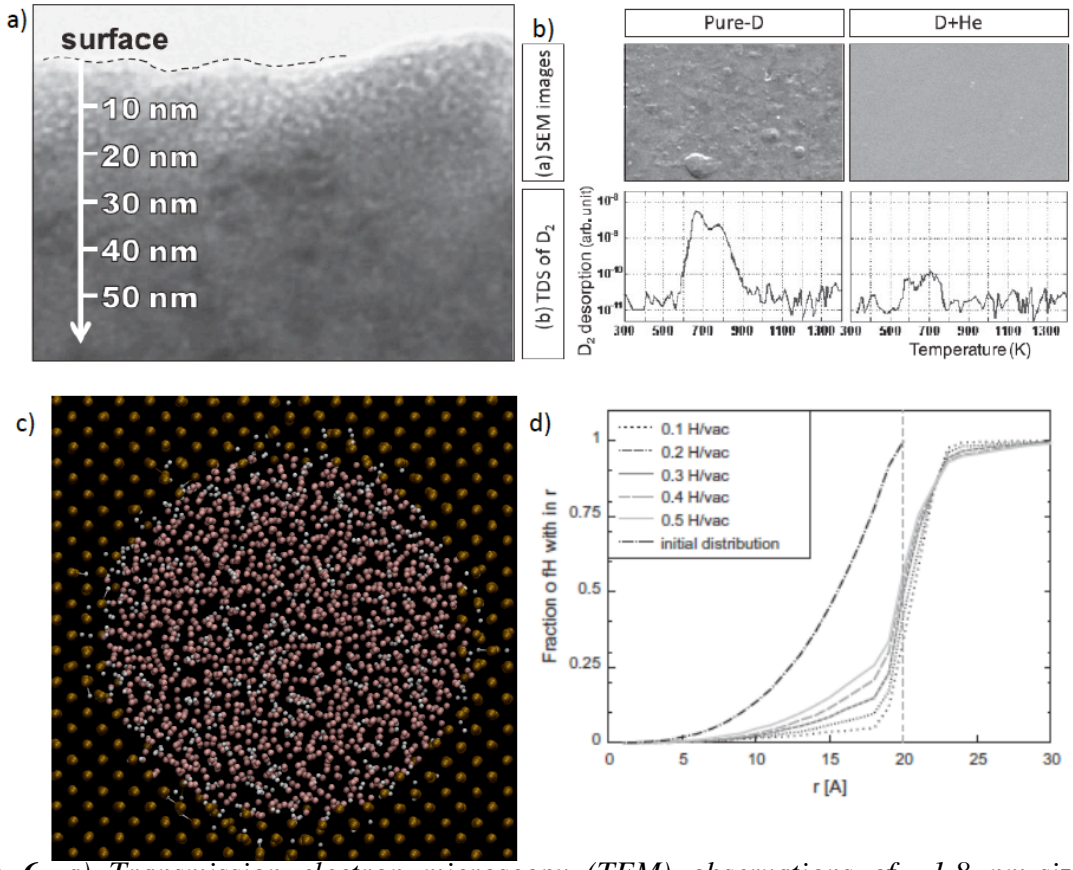

Figure 6. *a) Transmission electron microscopy (TEM) observations of ~1.8 nm-sized gas bubbles formed up to a depth of about 20 nm below a tungsten surface following exposure to a 60eV plasma containing 5%He-95%D at 200°C at an approximate implantation fluence of 10^{25} m^{-2}. b) Observation of the tungsten surface by scanning electron microscopy (SEM) for the same plasma conditions but comparing the effect of pure deuterium (D) plasma to that of 95%D-5%He, along with the measured deuterium desorption from tungsten samples between 300 and 1300K. c) Distribution of helium (pink) and hydrogen (white) atoms in a 2 nm radius gas bubble within tungsten (copper color), and d) quantitative distribution of the hydrogen within and outside of the bubble obtained from molecular dynamics (MD) simulations for a range of Hydrogen concentrations. Parts a) and b) have been reproduced from Ref. [24], while c) and d) are from Ref. [77].*